Cell Tissue Res (2000) 301:389–395
DOI 10.1007/s004410000241

REGULAR ARTICLE

P. Bodier-Houllé · P. Steuer · J. M. Meyer · L. Bigeard
F.J.G. Cuisinier

High-resolution electron-microscopic study of the relationship between human enamel and dentin crystals at the dentinoenamel junction

Received: 15 February 2000 / Accepted: 12 May 2000 / Published online: 4 July 2000
© Springer-Verlag 2000

Abstract The development of dentin and of enamel share a common starting locus: the dentinoenamel junction (DEJ). In this study the relationship between enamel and dentin crystals has been investigated in order to highlight the guiding or modulating role of the previously mineralized dentin layer during enamel formation. Observations were made with a high-resolution electron microscope and, after digitalization, image-analysis software was used to obtain digital diffractograms of individual crystals. In general no direct epitaxial growth of enamel crystals onto dentin crystals could be demonstrated. The absence of direct contact between the two kinds of crystals and the presence of amorphous areas within enamel particles at the junction with dentin crystals were always noted. Only in a few cases was the relationship between enamel and dentin crystals observed, which suggested a preorganization of the enamel matrix influenced by the dentin surface structure. This could be explained either by the existence of a proteinaceous continuum between enamel and dentin or by the orientation of enamel proteins by dentin crystals.

Key words Dentinoenamel junction · Structure · Mineralization · High-resolution electron microscopy · Numerical analysis · Human

Introduction

Dentin and enamel development share a common starting locus: the dentinoenamel junction (DEJ). Another important common characteristic of both tissues is the nature of their mineral crystals (Frank et al. 1960). Even if the size and the shape of dentin crystals are very different from those of enamel, both crystal types are constituted by carbonated, calcium-deficient hydroxyapatites (HAs; Brès et al. 1990; Schroeder and Frank 1985). These two characteristics were also considered as their only common property for a long time. Recent cellular biology data on the extracellular matrix (ECM) components and their expression in odontoblast and ameloblast cells showed complex relationships between both tissues (Nanci et al. 1994). The development of individual enamel and dentin crystals appeared, however, to be roughly comparable and was described in a four-step process (Houllé et al. 1997). The first two steps included the initial nucleation process and the formation of nanometer-sized particles. They were followed by ribbon-like crystal formation, which up until recently was considered as the first step of biological crystal formation (Cuisinier et al. 1995; Houllé et al. 1997). These complicated processes, starting with heterogeneous nucleation of inorganic calcium phosphate on an organic extracellular matrix, are controlled in both tissues by the organic matrix and are under cellular control (Mann 1993).

Enamel proteins are ephemeral and only a small amount of proteinaceous material remains in the adult tissue. The organic matrix of enamel is constituted by two major matrix proteins; the amelogenin and the nonamelogenin proteins (Zeichner-David et al. 1997). Amelogenins are also present in the developing mantle dentin. Amelogenin exists in the form of a liquid crystal mesophase, constituted in vitro and in vivo by nanospheres structurally stable at 37°C, and may be as a thixotropic gel implicated in the growth of enamel crystal (Moradian-Oldak et al. 1998). On images of developing enamel, amelogenins clearly appear to be organized in rows neighboring the c-axis of the ribbon-like enamel crystallites (Meyer et al. 1999). In dentin this function was devoted to type I collagen, which provides the physical support and the environment favoring mineral deposition (Weiner and Wagner et al. 1998). Amelogenins such as osteopontin in the case of bone crystal formation could also play a role in inhibition of crystal growth (Hunter et al. 1996). The role of the nonamelogenin pro-

P. Bodier-Houllé · P. Steuer · J.M. Meyer · L. Bigeard
F.J.G. Cuisinier (✉)
INSERM U 424, Fédération de Recherches Odontologiques, Université Louis Pasteur, 11 rue Humann, 67085 Strasbourg, France
e-mail: fred@odont3.u-strasbg.fr
Tel.: +33-388-243428, Fax: 33-388-243399

teins is not clearly defined, but it is widely accepted that they are involved in crystal nucleation, as suggested by their accumulation in crystal growth sites. The identification in the enamel matrix of a 70-kDa phosphorylated protein by a protein kinase (Salih et al. 1998) is perhaps also comparable with the presence in the dentin matrix of the dentin sialoprotein (DSP) phosphorylated by casein kinase (Sfeir and Veis 1996). It is tempting at this stage to suggest for both tissues that these two different proteins play similar roles with respect to the mineralization process.

Enamel crystals were described as growing either epitaxially on the preexisting dentin crystals because of a high continuity between enamel and dentin crystals (Arsenault and Robinson 1989; Hayashi 1993) or at a distance from the dentin surface (Diekwisch et al. 1998) followed by subsequent growth to bring them into contact with dentin crystals (Takano et al. 1996). The relationship between enamel and dentin should be thus investigated to highlight, during enamel formation, the guiding or modulating role of the previously mineralized dentin layer.

The aim of this work was thus to investigate the development of the DEJ using high-resolution electron microscopy (HREM). We focused our attention on the relationship between enamel and dentin crystals and on the function of organic matrices in DEJ formation. Our intimate knowledge of both enamel (Cuisinier et al. 1992, 1993) and dentin crystal growth processes (Bodier-Houllé et al. 1998; Houllé et al. 1997) was a useful prerequisite in the investigation of such a complex relationship.

Materials and methods

Specimen preparation

The specimens (incisors) were collected from 5-month-old human fetuses (Gynecological Department, Université Louis Pasteur, Strasbourg, France) according to a protocol conforming to university standards. They were fixed for 3 h in a 2% glutaraldehyde and 2% paraformaldehyde solution in 0.1 M sodium cacodylate buffer, pH 7.4. After 2 h postfixation in 1% OsO_4 solution in the same buffer, the specimens were embedded in Epon 812.

Nondecalcified, ultrathin sections were obtained with an MT-2b Sorvall-Porter (Newtown, USA) microtome equipped with a diamond knife. The sections were floated on water saturated against HA (200 $mg.l^{-1}$) by Biogel HTP HA (Biorad, Richmond, USA), in order to prevent crystal dissolution.

High-resolution electron microscopy

The unstained sections were observed in a transmission electron microscope (Philips EM 430 ST, Eindhoven, The Netherlands) operating at 300 kV, using a double-tilt specimen holder and a nitrogen-cooled anticontamination device. The microscope possesses a spherical aberration constant of 1.1 mm and a Scherzer resolution of 0.19 nm. The micrographs were recorded on SO163 films (Kodak, Rochester, USA). For each selected image, the absence of astigmatism and drift was checked by optical diffraction on an optical bench (Micro-contrôle, Evry, France).

Image digitalization

The micrographs were digitized by the SERTIT (Service Regional de Traitement d'Image et de Télédétection, Strasbourg, France). A very high resolution drum microdensitometer (Wirth 105D, Frankfurt am Main, Germany) with analysis steps of 25 µm was used. For deeper analyses, the images were then transferred onto a Silicon Graphics Indigo-2 station (Silicon Graphics, Mountain View, USA).

Image analyses

The numerical analyses were realized with a Khoros software package (Khoral Research, Albuquerque, New Mexico, USA). The Khoros programs allow information processes, data exploration, and visualization. The programs, as well as the library, are presented in toolboxes. Multidimensional operators were used for data handling such as arithmetic calculation, data conversion, data organization, and size treatment, and some others to visualize the images such as an image presentation program and animation program. We used Khoros software mainly to select a small area inside the crystals and to perform fast Fourier transform (FFT) of these selected areas. The FFT algorithm allowed us to work on rectangular images.

Results

The low-magnification (LM) image analysis was of great importance in understanding crystal organization in the DEJ, whereas high-magnification (HM) images were essential to perform structural analyses.

At LM the junction between enamel and dentin appears to be irregular (Fig. 1), and it was quite easy to

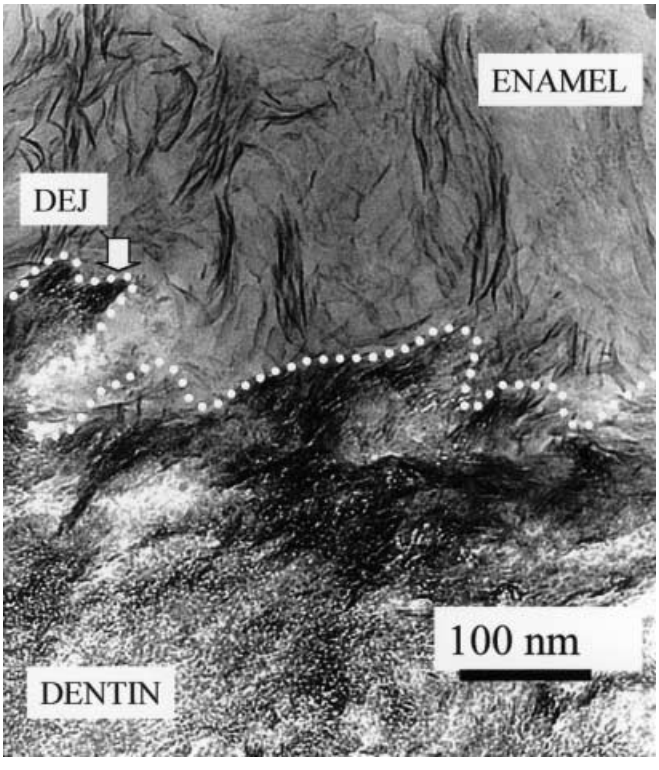

Fig. 1 Low magnification of the human dentinoenamel junction (DEJ), delineated by a *white dotted line*

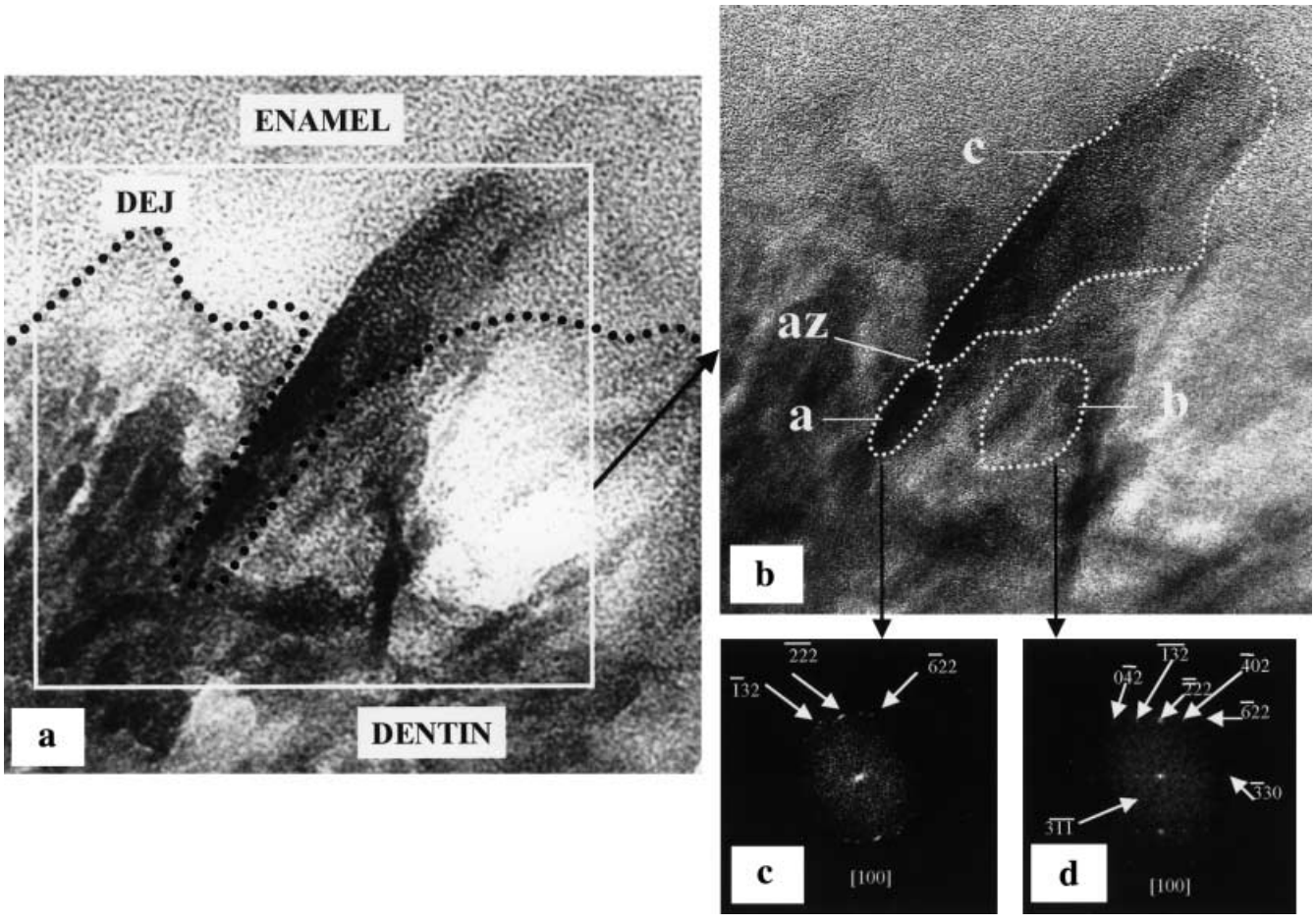

Fig. 2 **a** Low-magnification (LM) image of the DEJ, indicated by the *dark dotted line*. In the window delimited by the *white line*, an enamel crystal emerging from the dentin surface can be seen. **b** High-magnification (HM) image of the same area. (HM is not an enlargement of LM). The HM image corresponds to the window selected in the LM image. Areas *a* and *c* correspond to enamel particles and *b* to a dentin crystal. **c** Numerical diffractogram corresponding to particle *a*. Zone axis [100]. **d** Numerical diffractogram corresponding to particle *b*. Zone axis [100]

locate the frontier between both areas. Owing to the weak contrast at HM (×500,000 on the microscope screen) and to the small size of the observed area, it was very difficult (and absolutely unrealistic) to try to determine which particle belongs to dentin or to enamel. For this reason, we have always combined LM and HM images in our figures to locate the DEJ precisely. At LM it was also possible to distinguish the dentin from enamel crystals by their shape. The dentin crystals appeared to be round, small, and apparently randomly distributed, whereas enamel crystals possessed ribbon-like habits, with longer and larger sizes. In given domains, they exhibited a parallel orientation and a darker contrast. Enamel crystals seem to emerge from the dentin surface, and no clear separation between both crystals was seen at the DEJ. Further from the DEJ, the discrimination between dentin and enamel crystals was obvious.

The DEJ area at LM is clearly visible in Fig. 2a. The enamel particles presented a typical dark contrast that, at first sight, could be assimilated to a better mineralized state than dentin particles. The dentin particles were also smaller and less dark. On a HM image of the same area (Fig. 2b), we observed an enamel crystal constituted by two particles (a and c) separated by a thin, clear amorphous zone (az). The numerical diffractogram of particle a (Figs. 2, 3) shows that the observation axis was [100]. The numerical diffractogram of particle c, with an absence of dots (not presented), was due to completely amorphous material. This showed that the (dark) contrast of particle c was not related to a crystallized state. The contrast of the LM observations then suggested the presence of a thick organic matrix and/or a high local concentration of atoms, as in the case where amorphous apatite material is present. Owing to the imaging conditions used, the image contrast results from electron absorption, more precisely from a quantity proportional to the atomic potential (Spence 1988). The shapes of particles a and c were comparable with the ribbon-like habit of a secretory enamel crystal. The well-defined border suggested that the dark contrast could result from the deposition of calcium phosphate atoms in an amorphous state onto an organic substrate. This step could thus constitute an intermediate situation before a better-organized crystallization. The numerical diffractogram (Fig. 2d) of particle b,

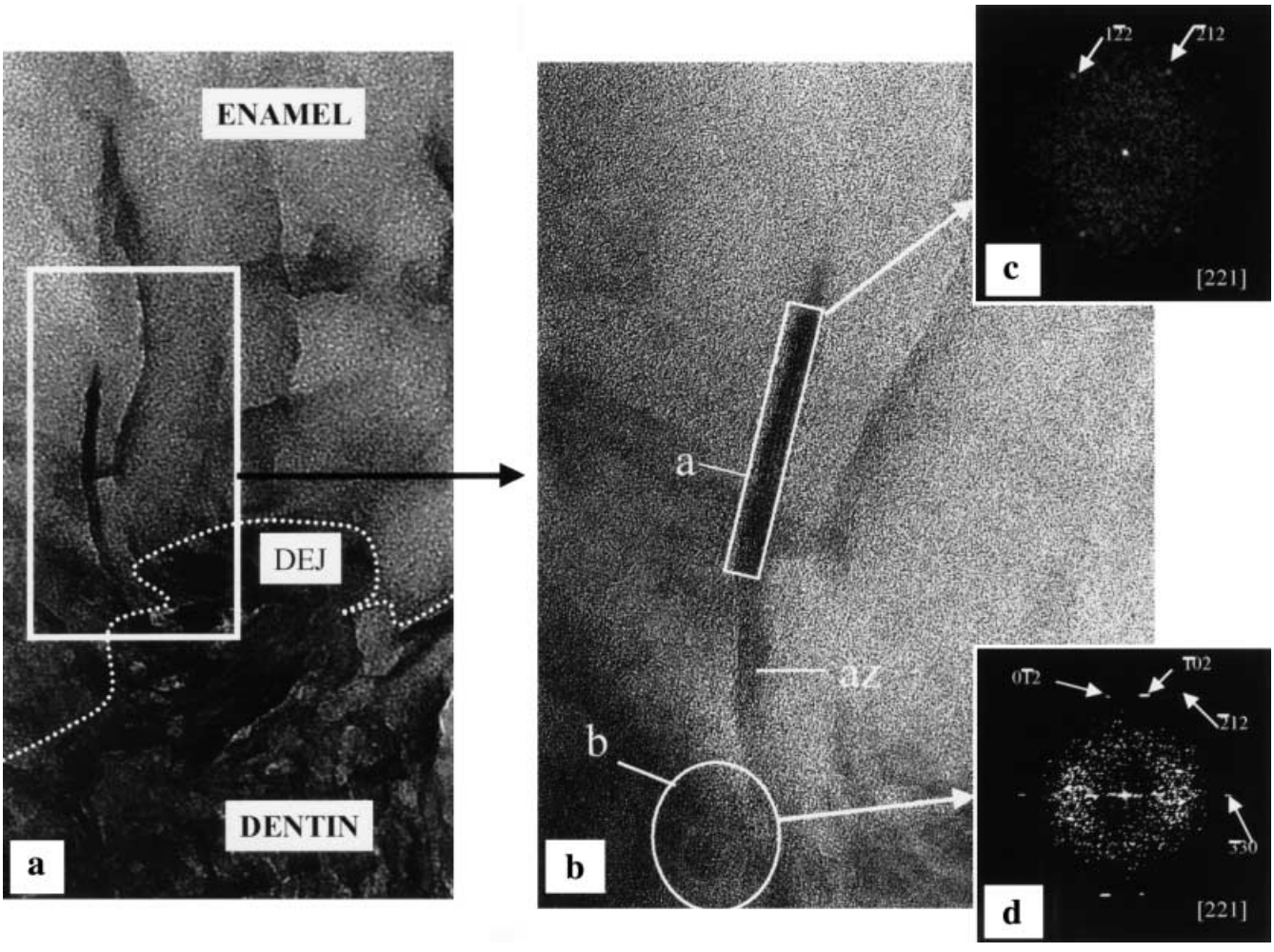

Fig. 3 **a** LM image of the DEJ, indicated by the *white dotted line*. In the window delimited by a *white line*, an enamel crystal can be seen (*dark contrast*) emerging from the dentin. The HM image corresponds to the window selected in the LM image. **b** HM image of the same area; *az* and *a* correspond to two areas of the enamel particle observed in a. The area in the *white circle* corresponds to a dentin crystal (*b*). **c** Numerical diffractogram of enamel area *a*, which is observed along the [221] zone axis. **d** Numerical diffractogram of dentin crystal *b* observed along the [221] zone axis

which belonged to the dentin domain, showed diffraction spots characteristic for the [100] zone axis of hydroxyapatite (HA). The two particles a and b were thus observed with the same zone axis, indicating that they possess a common orientation along the [100] axis. Particle orientation in the plane perpendicular to the [100] axis, i.e., the {100} plane, was estimated by determining the orientation of the <001> planes of both diffractograms. The angular difference was of 3.9°. Such a small disorientation was close to the disorientation generally observed for epitaxial growth. Thus by a subsequent growth both particles could come in close contact and a small angle grain boundary could be formed.

In the case of the DEJ shown in Fig. 3a, the long ribbon-like habit of the particles constituted also characteristics of the enamel crystals in the secretory formation stage (Cuisinier et al. 1992).

This enamel particle appeared homogeneous and curved (white box in Fig. 3a). The same particle on the HM image seemed to be formed by two different areas (Fig. 3b). The area az, which is close to dentin, is completely amorphous, whereas the other part (a in Fig. 3b) possessed a crystalline structure. The numerical diffractogram in Fig. 3c of crystal a indicated that the crystal was observed along the [221] zone axis of HA. In the close vicinity of the enamel particle extremity az, we observed also a small dentin particle b (Fig. 3b). The numerical diffractogram in Fig. 3d of this small b particle showed also the characteristic spots of the [221] zone axis of HA. The orientation of the two crystals (a and b) in the plane perpendicular to the [221] axis was determined by measuring the angle between the <$\bar{2}$12> planes on each numerical diffractogram (Fig. 3c,d). The angle formed was 16°. The curved morphology of the enamel particle and the long distance between areas a and b separated by the az zone certainly contributed to this large angular value. Such a high angular disorientation angle is practically incompatible with an epitaxial relation between particles a and b. This observation was also strengthened by the long distance between both crystals.

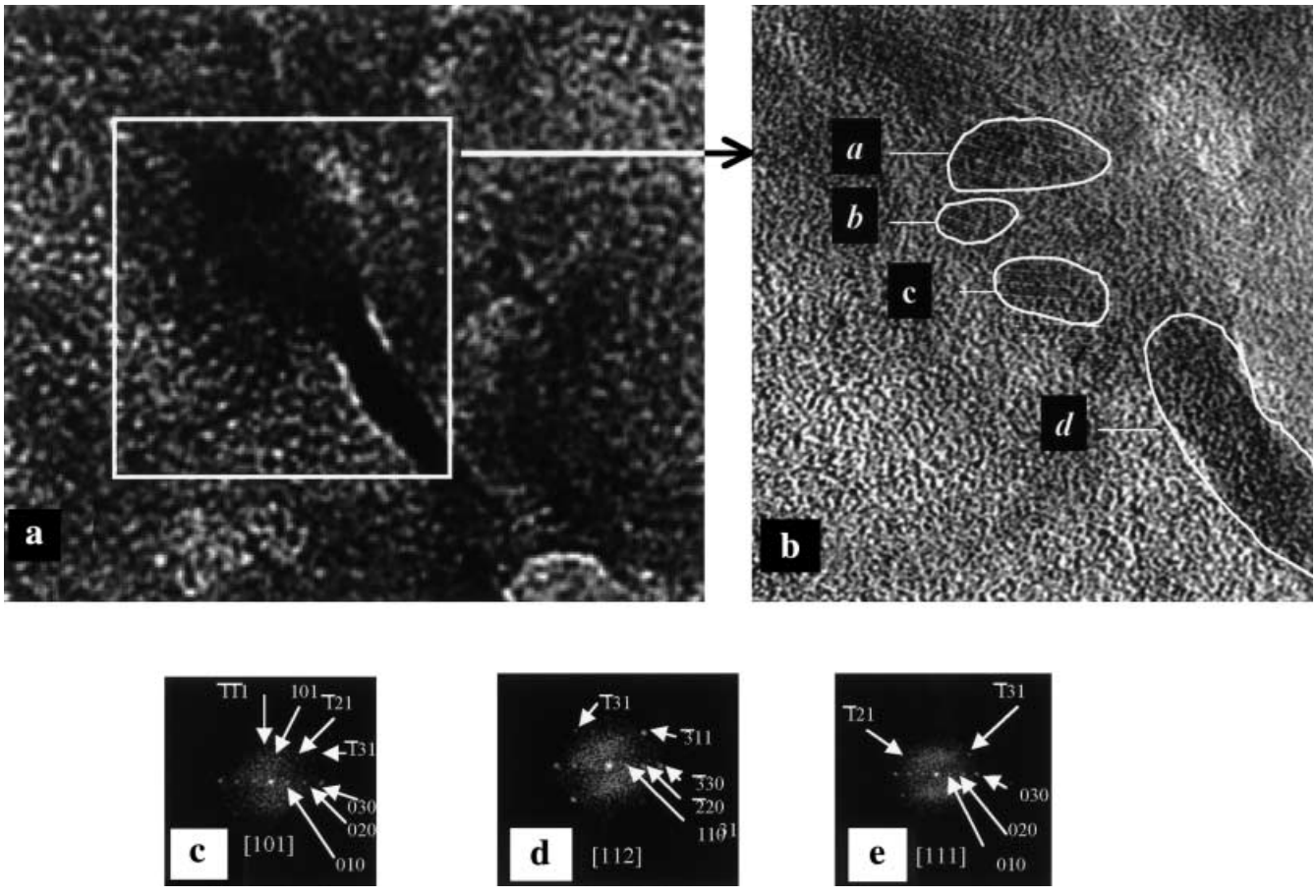

Fig. 4 **a** LM image of DEJ; **b** HM image of DEJ (*a–c* dentin crystals, *d* enamel particle). **c** Numerical diffractogram of particle *a*, observed along the [101] zone axis. **d** Numerical diffractogram of particle *b*, observed along the [112] zone axis. **e** Numerical diffractogram of particle *c*, observed along the [111] zone

Two different images of the same DEJ are given in Fig. 4. The LM image (Fig. 4a) shows the dark contrast of an enamel crystal. Crystal d (Fig. 4b) seems to emerge from the dentin and its long needle-like habit was rather characteristic for the enamel tissue. On the HM image, the three particles termed "a, b, c" corresponded to dentin-like structures due to their dot-like aspect and their more random arrangement. Their numerical diffractograms (Fig. 4a,b,c) indicated that they were observed along the [101], [112], and [111] zone axes, respectively. Particle d (Fig. 4b), apparently completely amorphous, corresponded to an enamel particle because of its ribbon like habit; it had no crystalline arrangement. In this specific area, no structural relationships between enamel particles and the surrounding dentin crystals were found.

Discussion

The first main point that emerged from the careful LM image analyses of the enamel and dentin crystallites in the DEJ was the density and darkness of the enamel crystals not necessarily related to a fully organized crystalline structure. Enamel ribbon-like particles, which appeared dark and uniform in LM images, actually showed different features on HM images, corresponding either to amorphous or crystalline structures. This aspect implies the presence of amorphous material zones in the very early developmental stages.

In LM observations, the contrast resulted from the electron absorption by the specimen and it was enhanced by the strong defocalization of the objective lens of the microscope (Spence 1988). The interactions between electrons and specimen, therefore the absorption too, are proportional to the atomic potential of the specimen. Under such conditions, the contrast can be due mainly to a local accumulation of heavy atoms of different origins. While specimens were observed without staining, the contrast could not be related to accumulation of uranyl or lead atoms. The only possible staining procedure was OsO_4 postfixation. In the present case, we can thus also suggest that calcium and phosphate ions can also be involved in the contrast formation. Due to the important image density, this would also suggest the presence of a high local concentration of calcium and phosphate ions. The well-defined shape and the tissue-specific habit (ribbon-like) of the particles suggest also that this accumulation is well controlled and could perhaps occur on an organic substrate.

Both observations seem to indicate clearly that the dark structures are not due to electron-microscopic arti-

facts. The calcium and phosphate ions accumulated on the substrate are often in an amorphous state, as demonstrated by the numerical diffraction of some enamel particles. At this point, however, we have also to define amorphous material precisely, which is characterized by the absence of long-range order dimensions (Bursill et al. 1981). In contrast to this, a material with short-range order dimensions could be formed by small crystals of a few nanometers. Earlier we described such nanometer-sized particles in enamel (Cuisinier et al. 1993). In this study, nanometer-sized particles were not observed close to the enamel crystallites found at the DEJ. The fact that no amorphous precursor was detected previously in enamel tissues shows that amorphous states have a short life span before conversion into crystallized calcium phosphate. Such amorphous materials could be related to a precursor mineral phase. Two main theories have been advanced to explain the formation of HA crystals in biological tissues. The first one explains bone crystal formation as a continuous mechanism in which a poorly crystallized HA (PCHA) was transformed to well-crystallized HA. The second theory is based upon the existence of a precursor mineral phase. The two most prominent precursors that have been considered are octacalcium phosphate (OCP; Bodier-Houllé et al. 1998; Brown 1965) and amorphous calcium phosphate (ACP; Glimcher et al. 1981). Electron-microprobe analysis could not be considered for the determination of the nature of the growing crystals due to the semi-quantitative nature of the measurements. Such transformations from amorphous to crystallized states were also described for calcium carbonate mineralization (Beniah et al. 1997).

The enamel crystal growing steps at the DEJ are a matter of considerable debate. Some authors claim that the enamel crystals grow epitaxially on the preexisting dentin crystals because of a high continuity between enamel and dentin crystals (Arsenault and Robinson 1989; Hayashi 1993). Others have shown that enamel crystals are formed at a given distance from the dentin surface (Diekwisch et al. 1998) and could either reach dentin crystals by a subsequent growth (Takano et al. 1996) or remain distant (Dong and Warshawsky 1996). In the present study, we found only two types of crystallographic orientations between enamel and dentin crystals, and in both cases no direct contact between particle types was found (Figs. 2, 3). Owing to the small number of observations and the difficulties in clearly identifying enamel or dentin crystals at such early developmental stages, the proposed interpretations must be received with caution. The presence of low- and high-angle disorientations between dentin and enamel particles could indicate epitaxial relations between certain particles. However, this hypothesis cannot be confirmed because of the absence of direct contact between the crystals. In contrast, the existence of amorphous domains within enamel particles in the close vicinity of the dentin crystals suggests the absence of an epitaxial growth.

The presence of amorphous areas in enamel particles at the junction with dentin crystals shows the existence of different temporal events. One could thus speculate that at the beginning of the process an organic substrate must be present onto which calcium and phosphate accumulate, and that later on a progressive, inorganic phase transformation from an amorphous to a crystalline state could occur. In the case of an epitaxial growth mechanism for enamel crystals on dentin crystals, the crystallization must directly start on the dentin crystal surface. The enamel crystal formed under such conditions would thus be homogeneously crystallized, with no amorphous area between the two zones. Such an epitaxial growth mechanism would also completely exclude any role of the organic matrix in the control of the enamel crystal formation at the DEJ.

In conclusion our observations strongly suggest that no epitaxial growth of enamel crystals on dentin crystals occurs. The small disorientation angles found between enamel and dentin crystals could be simply a result of the preorganization of the enamel extracellular matrix under the influence of dentin components. This also implies interactions between both tissue types. Such preorganization can result from different mechanisms. It is well documented that amelogenins are secreted by ameloblasts and are present during DEJ mineralization in both tissues (Nanci et al. 1994). The mineralization of the outer dentin layer could induce an immobilization of amelogenins. This could constitute fixed starting points for the formation of supramolecular nanosphere columns. In the case of anionic enamel proteins, a consensus exists on their possible involvement in the heterogeneous nucleation process of enamel crystals. Uncleaved enamelin is believed to constitute a nucleation substrate during crystal elongation (Hu et al. 1997). Our observations are compatible with the existence of a protein layer on which calcium and phosphate accumulate. The main question arising is the nature of the relationship between this enamel organic substrate and the dentin components. An elaborate hypothesis concerns the existence of specific interactions between enamel anionic proteins and dentin crystals. It has been demonstrated that proteins have a high affinity for apatite crystal surfaces, especially HA surfaces (Kandori et al. 1995). Such mineral surfaces could act as sites for supramolecular self-arrangement of matrix proteins (Schwartz 1996). We could then postulate the existence of an assembly and a linkage between the dentin crystal surface and immature proteins originating from ameloblasts. These new aspects of enamel formation should provide new clues for cell biologists in determining the functions of enamel and dentin proteins.

References

Arsenault AL, Robinson BW (1989) The dentino-enamel junction: a structural and microanalytical study of early mineralization. Calcif Tissue Int 45:111–121

Beniah E, Aizenberg J, Addadi L, Weiner S (1997) Amorphous calcium carbonate transforms into calcite during sea urchin larval spicule growth. Proc R Soc Lond B Biol Sci 264:461–465

Bodier-Houllé P, Steuer P, Voegel JC, Cuisinier FJG (1998) First experimental evidence for human dentin crystal formation involving conversion of octacalcium phosphate to hydroxyapatite. Acta Crystallogr D 54:1377–1381

Brès EF, Voegel JC, Frank RM (1990) High-resolution electron microscopy of human enamel crystals. J Microsc 160:183–201

Brown WE (1965) A mechanism for growth of apatitic crystals. In: Stack MV, Fearnhead RW (eds) Tooth enamel, vol I. Wright, Bristol, pp 11–14

Bursill LA, Mallinson LG, Elliott SR, Thomas JM (1981) Computer simulation and interpretation of electron-microscopic images of amorphous structures. J Phys Chem 85:3004–3006

Cuisinier FJG, Steuer P, Senger B, Voegel JC, Frank RM (1992) Human amelogenesis. I. High-resolution electron microscopy of ribbon-like crystals. Calcif Tissue Int 51:259–268

Cuisinier FJG, Steuer P, Senger B, Voegel JC, Frank RM (1993) Human amelogenesis: high-resolution electron microscopy of nanometer-sized particles. Cell Tissue Res 273:175–182

Cuisinier FJG, Steuer P, Brisson A, Voegel JC (1995) High-resolution electron microscopy study of chicken bone crystal growth mechanisms. J Crystal Growth 156:443–453

Diekwisch TG, Berman BJ, Genters S, Slavkin HC (1998) Initial enamel crystals are not spatially associated with mineralized dentin. Cell Tissue Res 279:149–167

Dong W, Warshawsky H (1996) Lattice fringe continuity in the absence of crystal continuity in enamel. Adv Dent Res 10(2):232–237

Frank RM, Sognnaes RF, Kerns R (1960) Calcification of dental tissues with special reference to enamel structure. In: Calcification in biological systems. AAAS, Washington DC, pp 163–202

Glimcher MJ, Bonar LC, Grynpas MD, Landis WJ, Roufosse AH (1981) Recent studies of bone mineral: is the amorphous calcium phosphate theory valid ? J Cryst Growth 53:100–119

Hayashi Y (1993) High-resolution electron-microscopic study of the human dentin crystal. J Electron Microsc 42:141–146

Houllé P, Voegel JC, Schultz P, Cuisinier FJG (1997) High-resolution electron microscopy: structure and growth mechanisms of human dentin crystals. J Dent Res 76:895–904

Hu CC, Fukae M, Uchida T, Qian Q, Zhang CH, Ryu OH, Tanabe T, Yamakoshi Y, Murakami C, Dohi N, Shimizu M, Simmer JP (1997) Cloning and characterization of porcine enamelin mRNAs. J Dent Res 76(11):1720–1729

Hunter GK, Hauschka PV, Poole AR, Rosenberg LC, Goldberg HA (1996) Nucleation and inhibition of hydroxyapatite formation by mineralized tissue proteins. Biochem J 317:59–64

Kandori K, Shimizu T, Yasukawa A, Ishikawa T (1995) Adsorption of bovine serum albumin onto synthetic calcium hydroxyapatite: influence of particle texture. Colloids Surf B Biointerfaces 5:81–87

Mann S (1993) Molecular tectonics in biomineralization and biomimetic materials chemistry. Nature 365:499–505

Meyer JM, Bodier-Houllé P, Cuisinier FJG, Lesot H, Ruch JV (1999) Initial aspects of mineralization at the dentino-enamel junction in embryonic mouse incisor in vivo and in vitro: a TEM comparative study. In Vitro Cell Dev Biol Anim 35(3):159–68

Moradian-Oldak J, Leung W, Fincham AG (1998) Temperature and pH-dependent supramolecular self-assembly of amelogenin molecules: a dynamic light-scattering analysis. J Struct Biol 122(3):320–327

Nanci A, Kawaguchi H, Kogaya Y (1994) Ultrastructural studies and immunolocalization of enamel proteins in rodent secretory stage ameloblasts processed by various cryofixation methods. Anat Rec 238:425–436

Salih E, Huang J, Gouverneur M, Glimcher M (1998) Enamel phosphoproteins and protein kinases: novel methods in the determination of covalently bound phosphates and their topographical distribution. 6th Int Conf Chem Biol Mineralized Tissues. Vittel, France

Schroeder I, Frank RM (1985) High-resolution electron microscopy of adult human peritubular dentin. Cell Tissue Res 242:449–451

Schwartz AW (1996) Did minerals perform prebiotic combinatorial chemistry? Chem Biol 3:515–518

Sfeir C, Veis A (1996) The membrane associated kinases which phosphorylate bone and dentin extracellular matrix phosphoproteins are isoforms of cytosolic CKII. Connect Tissue Res 35(1–4):215–222

Spence JCH (1988) Experimental high-resolution electron microscopy. Oxford University Press, Oxford

Takano Y, Hanaizumi Y, Oshima H (1996) Occurrence of amorphous and crystalline mineral deposits at the epithelial-mesenchymal interface of incisors in the calcium-loaded rat: implication of novel calcium binding domains. Anat Rec 245:174–185

Weiner S, Wagner HD (1998) The material bone: structure-mechanical function relations. Annu Rev Mater Sci 28:271–298

Zeichner-David M, Vo H, Tan H, Diekwisch T, Berman B, Thiemann F, Alcocer MD, Hsu P, Wang T, Eyna J, Caton J, Slavkin HC, MacDougall M (1997) Timing of the expression of enamel gene products during mouse tooth development. Int J Dev Biol 41:27–38